Reinforced concrete cover cracking due to the pressure of corrosion products

A. Muñoz & C. Andrade
Institute of Science Construction Eduardo Torroja, Madrid, Spain
A. Torres
Mexican Transport Institute, Queretaro, Mexico

ABSTRACT: Reinforcement corrosion is one of the most important phenomena that reduce the service life of the reinforced concrete structures. Steel corrosion reduces the strength and bond of the reinforcement and the oxides formed cause internal stresses that crack the concrete cover. The prediction of the evolution of these effects is a problem that involves chemical and mechanical aspects. The phenomenon is not well known and quantitative descriptions of development and magnitude of stresses produced by a corroding rebar to concrete are scarce and although there are several models in the literature they do not universally reproduce the experimental results. This work presents a summary of the available experimental evidence on the amount of internal expansion needed at the reinforcement level for concrete cover to crack and formulas to estimate the expansion. Also, results are presented on the pressure needed for concrete cover to crack together with the experimental technique used for the verification of the assumptions and crack propagation analysis.

1 INTRODUCTION

The steel reinforcement is protected from corrosion by passivation due to the high alkaline environment provided by the cement hydration. However, in the marine ambient chloride ions from seawater accumulate on the surface of the concrete and slowly diffuse through the concrete cover to the underlying steel. When the chloride ion concentration at the rebar depth exceeds a critical threshold value, the protective passive layer on the steel surface breaks down and active steel corrosion begins.

The transformation from steel to corrosion products in concrete is only partially understood. Analytical techniques cannot be used in situ to determine the type of corrosion products generated at the embedded rebar surface without exposing the rebar to the exterior. Furthermore corrosion products may oxidize upon exposing the rebar to air. Although discrepancies on the type of corrosion products formed at the steel/concrete interface are still present (Bedu 1993, Fontana 1986, Sagoe-Crentsil & Glasser 1989a, b, 1993), it appears nevertheless well established that these corrosion products have smaller mass densities than steel (Tuutti 1982), resulting in volume expansion and concrete cover cracking.

The mechanical process of the corrosion product expansion due to corrosion is shown in Figure 1. The steel might be considered as a metal cylinder with an initial radius r_0, immersed in a semi-infinite concrete medium with a cover C, and undergoing corrosion only in the region L. As corrosion progresses, the radius decreases by an amount x (corrosion penetration). However, corrosion products occupy a volume that is larger than the original metal. The final volume increase corresponds to an increase Δ_{ref}, over the initial rebar radius, for a total value of $r_0+\Delta_{ref}$. The surrounding concrete is stressed by this effective radial expansion and provokes the concrete-cover cracking and spalling.

In the literature (Atimatay & Ferguson 1973, Bazant 1979a, b, Beeby 1983, Andrade et al. 1993a, Andrade et al. 1996, Alonso et al. 1994, Andrade et al. 1998), some experimental studies, theoretical investigations, and field observations of concrete cracking due to corrosion product expansion have been documented. However, fundamental aspects of the cracking mechanism essential for durability forecasting, remain unsolved.

As explained in the literature (Reinhardt 1984), rebar corrosion induces the development of internal stresses that may crack the concrete. However, quantitative descriptions of development and magnitude of stresses produced by a corroding rebar to concrete are scarce. Thus, further information on the relationship between corrosion expansion and internal pressure is desirable for modeling predictions.

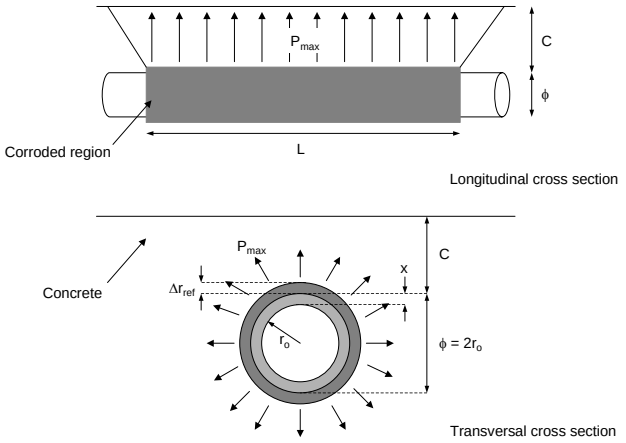

Figure 1: Corrosion process parameters.

The relation between the crack opening and the quantity of oxide generated by the corrosion expressed as the penetration of the corrosion or loss of diameter of the bars has been the subject of previous works by the authors by means of accelerated and not accelerated corrosion tests. One model (Leung 2001) obtains one upper and lower bound assuming the steel / concrete interface to be perfectly smooth or perfectly bonded. Some models (Andrade et al. 1993b, Martín-Perez 1998) assume a constant rate of rust production, while other models (Pantazopoulou & Papoulia 2001, Liu & Weyers 1995) analyze cracking time as a function of concrete cover, concrete and rust properties controlled by the rate of rust accumulation. Other papers develop models based on a critical corrosion attack penetration to initiate cracking and they relate it to the rebar radius (Torres 1999), steel cross section loss due to corrosion (Vidal et al. 2004) and cover / diameter ratio and concrete characteristics (Andrade et al. 1995, Rasheeduzzafar et al. 1992). Various numerical approaches use a finite element method analyzing cracking with the fixed smear crack model, assuming linear softening of the concrete (Padovan & Jae 1997), assuming linear elastic fracture mechanics and movable mesh placed around the crack tip to capture the local stress concentration (Ohtsu & Yoshimura 1997) and with the boundary element approach (Torres & Sagüés 2000). All calculations and the simulated cracking patterns of the papers are compared with experimental tests. It can be concluded, in general, that the beginning of the cracking depends principally on the relation between concrete cover thickness / diameter of the bars, the quality of the concrete and its tensile strength.

This work contributes to the study of the pressure needed to crack a certain cover and to confirm a predictive model for corrosion penetration taking into account specimen dimensions and fracture mechanic properties of the concrete.

2 EXPERIMENTAL WORK

2.1 *Materials and specimens*

The concrete mix was made with ordinary portland cement type II and the mix proportions (in kg/m^3) for each specimen are presented in the Table 1.

Table 1: Concrete mix proportions.

Material	Specimens	
	C1	P1, P2, P3
Cement	320	327
Max. Agg.	650	1016
Fine Agg.	1240	975
Water	200	165

The steel used was BS-500 having a 16 mm diameter. In the rebars of all specimens, four strain gauges were glued to measure the strain (pressure indirectly) at the steel-concrete interface. The specimen sizes are shown in the Figures 1 and 2. The specimens were cured for 24 hours in the moulds and 28 days in a curing room with 95% RH and 20º C. After the 28 day curing, the specimens were dried for some days to allow strain gauges at the concrete surface to reach the cracking moment. These were located as shown in Figures 2 and 3

2.2 *Accelerated corrosion and cracking test*

A 90 mm corrosion length was used for the C1 specimen and 230 mm for P1, P2 and P3. In order to activate the corrosion process, a 3% NaCl in cement weight were added to the mix and to accelerate the corrosion process, an electrical current (galvanostatic) was applied to the steel bar.

The accelerated corrosion procedure employed for the specimens consists in a galvanostat that applies a constant current density through the counter electrode placed at the ends of the specimens (Figure 2 and 3). The electric contact between the counter electrode and the concrete surface was provided by sponges maintained moistened by a water dropping system.

Three different current densities were used. Until the first crack appearance, the current densities were 1 (P1), 5 (P2) and 10 (C1 and P3) μA/cm^2 and after the first crack appearance the current densities were 10 (P1), 50 (P2) and 100 (C1 and P3) μA/cm^2 to follow the crack evolution.

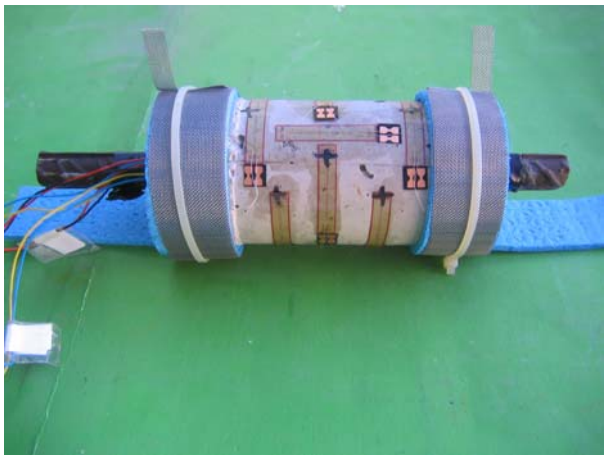

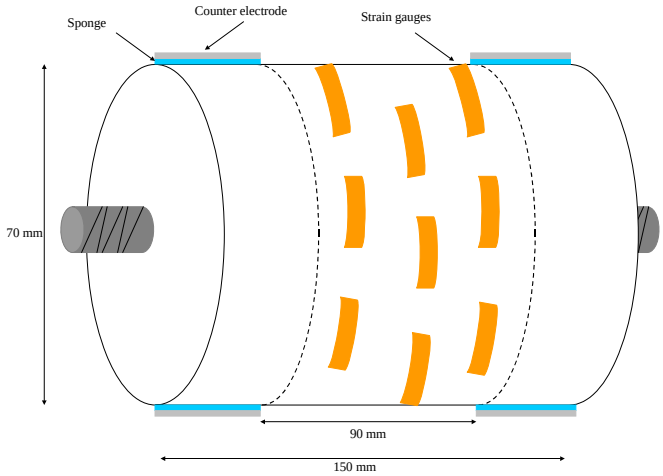

Figure 2: Cylinder C1 specimen.

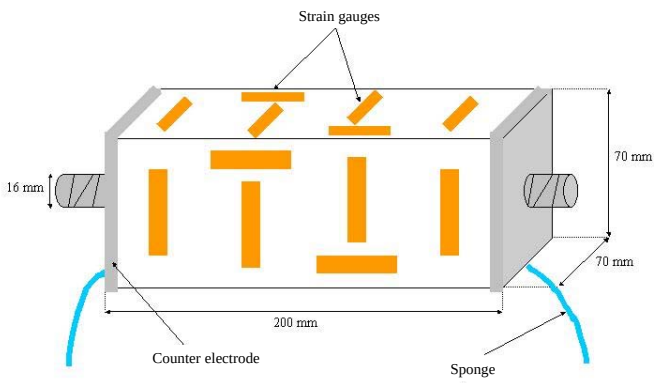

Figure 3: Prisms P1, P2 and P3.

The test is considered to end when a target cracking size is reached. After this, the specimens were disconnected from the corrosion equipment and were broken to study the types of oxides, the colors and their spread. Then, the bars were cleaned, dried and weighed to obtain the difference with respect to the initial weight (gravimetrical loss)

The conversion of corrosion rate into radius loss was performed using a formula based on Faraday's law (Andrade et al. 1993b):

$$P_x = 0.0116 \; I_{corr} \; t \qquad (1)$$

were x is the attack penetration in microns, I_{corr} is the current density in $\mu A/cm^2$, t is the elapsed time in years since the current was applied, and 0.0116 is a conversion factor of $\mu A/cm^2$ to µm/año in the case of homogeneous corrosion.

Preliminary, the radius losses were calculated by means of the expression (1). That is, all the current applied is assumed to be spent in the oxidation of the steel (100% of current efficiency is assumed). The losses so calculated are named "theoretical" steel losses. However, the 100% efficiency of the current was not produced and the "real" steel radius losses in every case were higher than the "theoretical" loss. This fact was verified by comparing the theoretical loss with the gravimetrical loss at the end of the tests.

3 RESULTS

3.1 *Expansion evolution*

Figure 4 shows the behavior of the strain gauges glued on the steel and the concrete surface of the C1 specimen. The gauge GM1 glued on the steel bar (Figure 4a) shows the most informative steel concrete interface stress behavior (by strain) due to the corrosion process. In the case of the gauges placed on the concrete surface (Figure 4b), it takes longer to show the expansion of gauges G3 and G9 where the first detecting the crack appearance.

For the case of prisms P1, P2 and P3 (Figures 5 to 7) the strain gauges glued on the steel bar (part a of Figures) measured similar behavior to the C1 specimen but the gauges placed on the concrete surface (part b of Figures) detect higher strains attributed to the swelling due to the permanent contact with the chloride solution. After 30 days, the gauges placed on the concrete surface showed more stability.

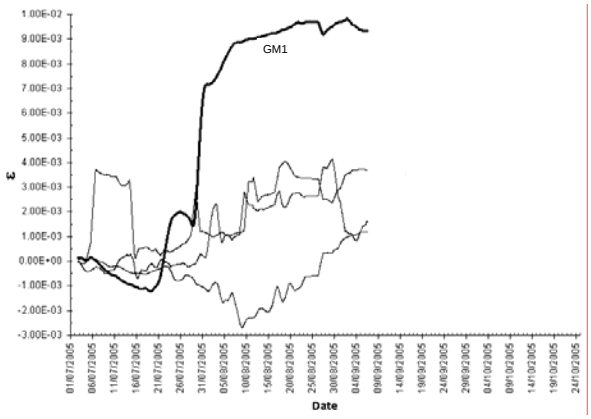

a)

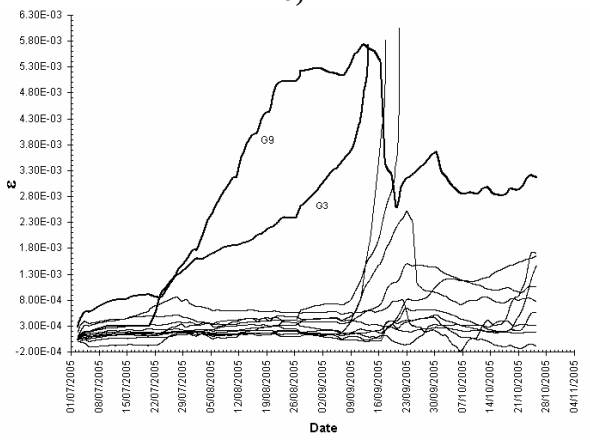

b)

Figure 4: a) Gauges GM glued on the steel bar and b) gauges G placed on the concrete surface of C1 specimen.

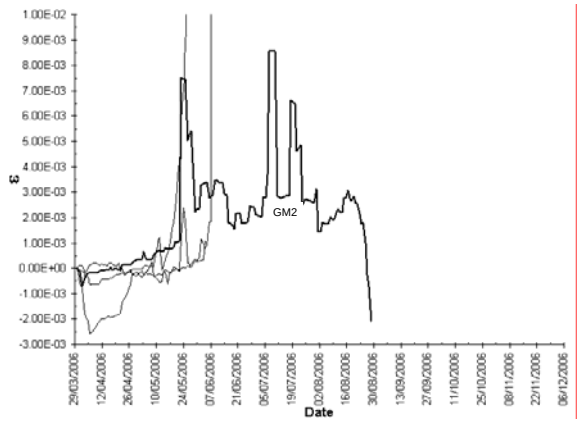

a)

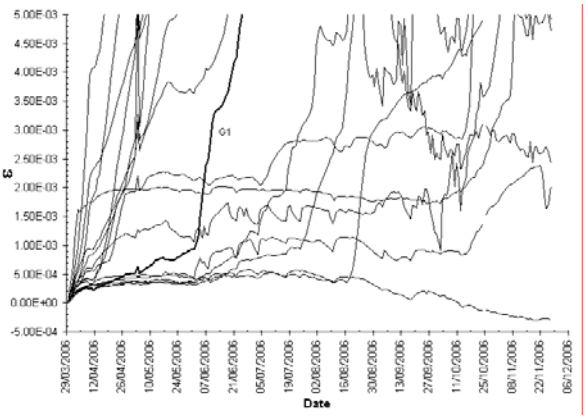

b)

Figure 6: a) Gauges GM glued on the steel bar and b) gauges G placed on the concrete surface of P2 specimen.

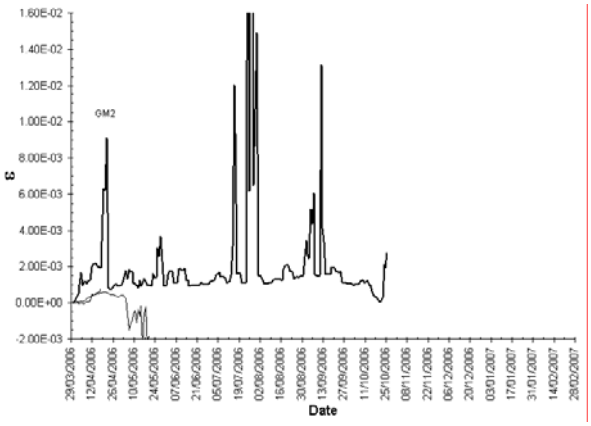

a)

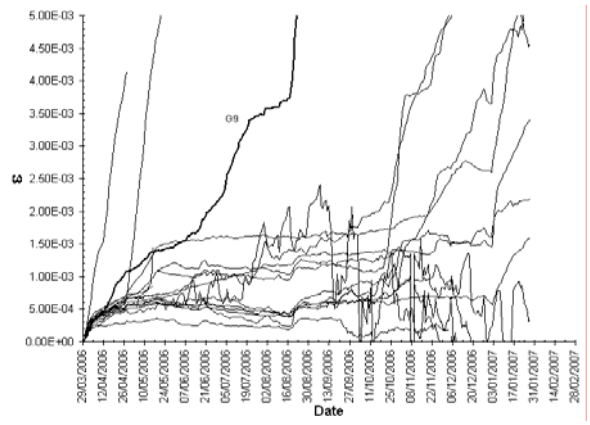

b)

Figure 5: a) Gauges GM glued on the steel bar and b) gauges G placed on the concrete surface of P1 specimen.

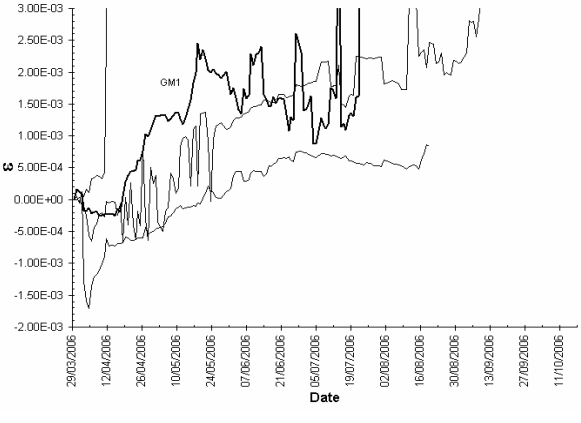

a)

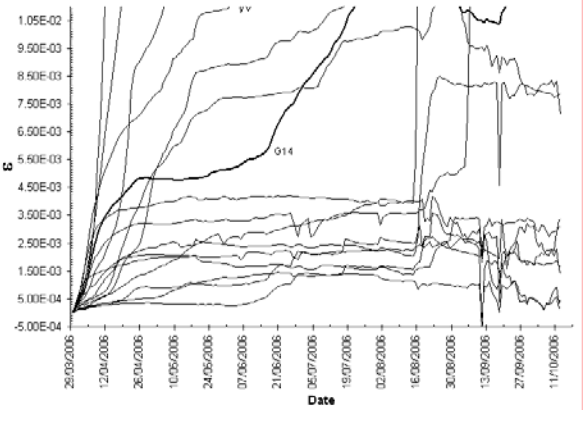

b)

Figure 7: a) Gauges GM glued on the steel bar and b) gauges G placed on the concrete surface of P3 specimen.

3.2 *Relation Attack penetration/cracking of concrete cover*

Previous investigations (Andrade et al. 1993a, Alonso et al. 1998) reported that the amount of corrosion needed to crack the concrete cover was only 15 to 50 microns for specimens with uniform corrosion, while the other author (Rodriguez et al. 1996) reports amounts of 50 to 140 microns for specimens with localized corrosion. For the tests carried out in this work, the corrosion penetration needed to crack the concrete cover of the specimens is shown in Table 2. The attack penetration results of P2 and P3 specimens are similar to the studies for specimens with uniform corrosion (Figure 8). While specimens C1 and P1 needed an even smaller amount of corrosion to crack.

Table 2: Corrosion penetration needed to crack the concrete cover.

Specimen	Attack penetration (μm)
C1	8.51
P1	4.26
P2	19.18
P3	34.78

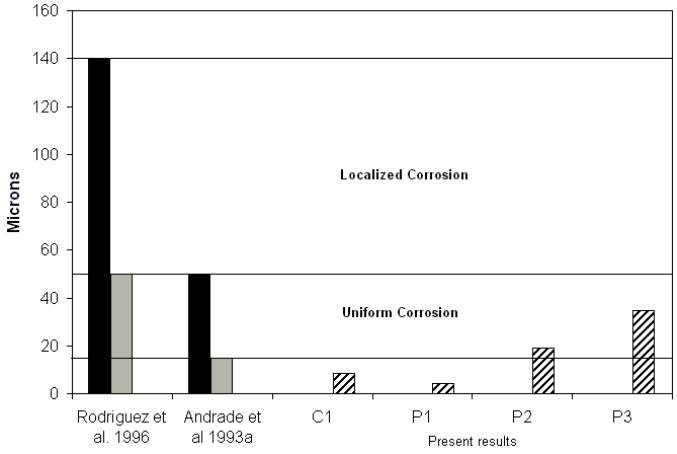

Figure 8: Amount of corrosion or attack penetration needed to crack the concrete cover; results of this work compared and results of other authors.

4 DISCUSSION

4.1 *Test methodology*

The strain gauges glued on the steel bar and placed on the concrete surface is a common technique used to try to detect the concrete cover cracking initiation (Andrade et al 1993a, b and Torres 1999). The results presented in this work confirm that the strain gauge test methodology can give important information to estimate the pressure needed to initiate the concrete cover cracking, but it is important to mention that not all the gauges work correctly. The temperature and humidity can affect the correct behavior of the gauges and the measurements can give erroneous information.

4.2 *Amount of corrosion needed to crack the concrete cover*

There are some models to estimate the corrosion amount needed to crack the concrete cover in the bibliography (Rasheeduzzafar et al. 1992, Andrade et al. 1993b, Liu & Weyers 1995, Rodriguez et al. 1996, Ohtsu & Yoshimura 1997, Padovan & Jae 1997, Martin-Perez B. 1998, Torres 1999, Leung 2001, Pantazopoulou & Papoulia 2001, Vidal et al. 2004). Equations (2) and (3) given by Rodriguez et al. 1996 and Torres 1999 respectively are used to compare the theoretical values of the corrosion amount needed to crack the concrete cover with the results obtained in this paper. Equation (2) considers the cross section properties of the specimens and concrete tensile strength while Equation (3) considers only the cross section properties and the corrosion length.

$$P_{xo} = \left(83.8 + 7.4\frac{C}{\phi} - 22.6\, f_{ct,sp}\right)\cdot 10^{-3} \quad (2)$$

$$x_{crit} = 0.0111\ \frac{C}{\phi}\left(\frac{C}{L}+1\right)^{1.95} \quad (3)$$

where C is the concrete cover (mm), ϕ is the steel bar diameter (mm), L is the corrosion length (mm), P_{xo} is the corrosion amount needed to generate the first crack (mm) and $f_{c,sp}$ is the concrete splitting tensile strength (Kg/cm^2).

Table 3 shows the results of the corrosion amount needed to cracking initiation given by Equations (2) and (3) compared with the results obtained in this work.

Table 3: Results of corrosion amount estimated by Equations (2) and (3) with the results of this work.

	Amount of corrosion needed to first crack generation (microns)			
Eq.	C1	P1	P2	P3
2	31.87	35.36	35.36	35.36
3	31.24	23.62	23.98	23.77
real	8.51	4.26	19.18	34.78

The attack penetration by corrosion in the P3 specimen estimated with Equation (3) is similar to the real values obtained in the tests although Equation (3) is calibrated with localized corrosion results and the corrosion lengths were between 5 and 6 times greater approximately. The real attack penetration in P3 specimen is greater than the results obtained with Equation (2) but very similar to the results obtained with Equation (3). The attack penetration obtained in

the C1 specimen is smaller than the estimated values with Equations (2) and (3) which is attributed to the cylindrical section of C1 and to the low corrosion rate applied (1 μA/cm^2) in the P2 specimen.

4.3 *Pressure needed to concrete cover cracking*

To determine the pressure needed to crack the concrete cover P_r Equation (4) (Torres 1999), (5) (Sagüés et al. 1998) and (6), for a thick walled cylinder (Timoshenko 1989), were considered.

$$\frac{P_r}{f_t} = 1.54 \frac{C}{\phi}\left(\frac{C}{L}+1\right)^{0.72} \quad (4)$$

$$P_r = 1.5\left(\frac{C}{\phi}\right)^{0.85}\left(\frac{C}{L}+1\right) f_t \quad (5)$$

$$P_r = \frac{E\left(R_2{}^2 - R_1{}^2\right)\varepsilon}{R_2{}^2\ 2} \quad (5)$$

Where: f_t is the concrete tensile strength in kg/cm^2, C/ϕ is the cover/diameter ratio, C/L is the cover/length ratio, R_1 y R_2 are the internal radius (steel bar diameter) and external radius (specimen concrete cover) in mm, ε is the strain measured by the strain gauges placed in the concrete surface and E is the Young modulus for the concrete in kg/cm^2.

Table 4: Results of P_r in kg/cm^2.

Specimen	Periods	Strain gauges	P_r Ec. (4)	P_r Ec. (5)	P_r Ec. (6)
C1	1	GM1	**101.2**	**93.6**	**111.2**
		G3	**101.2**	**93.6**	29.0
	2	GM1	**101.2**	**93.6**	183.2
		G3	**101.2**	**93.6**	**115.4**
P1	1	GM2	**80.7**	**80.3**	**81.7**
		G9	**80.7**	**80.3**	43.6
	2	GM2	**80.7**	**80.3**	134.6
		G1	**80.7**	**80.3**	**136.6**
P3	1	GM2	**80.7**	**80.3**	**81.9**
		G1	**80.7**	**80.3**	34.2
	2	GM2	**80.7**	**80.3**	257.7
		G1	**80.7**	**80.3**	**298.6**
P4	1	GM1	**80.7**	**80.3**	**81.2**
		G14	**80.7**	**80.3**	452.8
	2	GM1	**80.7**	**80.3**	176.7
		G14	**80.7**	**80.3**	**799.5**

Table 4 shows the results obtained with Equations (4), (5) and (6) for the 4 specimens tested. The strain values with the GM1 strain gauge glued on the steel bar and the G3 strain gauge placed in the concrete surface were used to make the calculation with Equation (6) because both gauges detect the first crack appearance. The strain gauges GM1 and GM2 (for P3 and for P1 and P2 specimens respectively) were glued on the steel bar and gauges G9, G1 and 14 (for P1, P2 and P3 specimens respectively) placed on the concrete surface there were used too.

The strain data obtained with the gauges are considered in two periods as Table 4 shows. After 15 days of accelerated corrosion of specimen C1 the gauges GM1 and G3 measured considerable strain at the steel bar and the concrete surface (Figure 4). Following the gauge GM1 behavior, it was observed that it measured a "cracking" strain (P_r) at 30 days and is when assumes the maximum pressure produced on the concrete to generate the first crack (end of first period). Meanwhile, the gauge G3 continues the strain measure at the concrete surface. A gauge GM1 relaxation was observed after the 30 days indicating that the first crack generation at the interface and the corrosion products cannot maintain the same pressure because they fill the hollow generated by the crack. The second period ended when the first crack at the concrete surface appeared and the gauge G3 measured the maximum strain (after 60 days approximately).

The same procedure was followed for the P1, P2 and P3 specimen with the respective gauges mentioned before.

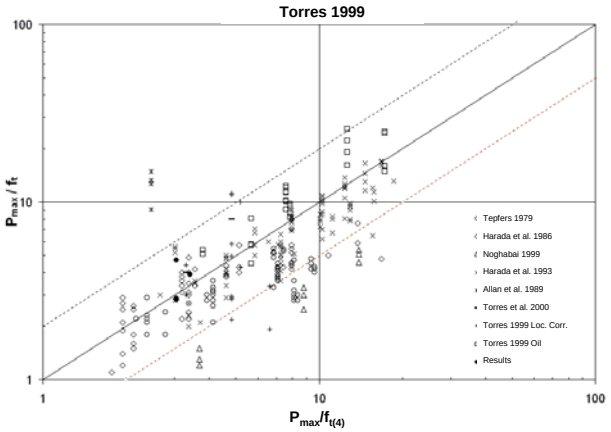

a)

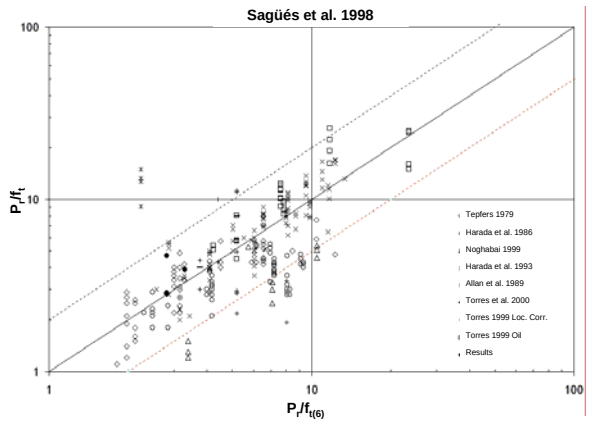

b)

Figure 9: Results P_r/f_t obtained with Equations (4) and (6) for some authors and test specimens.

Two models were chosen to estimate the pressure needed to crack the concrete cover. Those by Torres 1999 and Sagüés et al. 1998 (Equations (4) and (5)).

A comparison between the results of other authors and the results obtained in this paper of P_r/f_t estimated with Equations (4) and (6) are shown in Figure 9. The behavior of both models is similar but the results obtained with the model proposed by Torres 1999 is less scattered than the results obtained with the model proposed by Sagüés el al. 1998. The test results obtained with glued gauges in the steel bar and at the concrete surface of the specimen's technique and with uniform corrosion lengths remain in general model proposed trends.

5 CONCLUSIONS

The strain gauges glued on the steel bar and on the concrete surface of the test specimens provided good information to detect the concrete cover crack initiation period.

The galvanostatic procedure has proven to be an important tool in maintaining a constant rate of oxidation, although only the final gravimetrical losses can give reliable results.

The corrosion rate has a very significant influence on the limits of attack penetration to generate the first crack. A slower corrosion rate generates earlier cracking with lower attack penetrations.

From the test carried out in this work it is confirmed that the attack penetration or radius losses of 10-50 μm are necessary to generate crack widths of 0.05-0.1 mm.

Finally, the maximum pressure needed to crack the concrete cover can be estimated with the data obtained by the gauges and the models proposed. This pressure reported to be in present assumed 80 to 100 kg/cm^2.

REFERENCES

Allan, M. L. & Cherry, B. W. 1989. Mechanical simulation of corrosion induced cracking in reinforced concrete, *Corrosion/89*, Conference paper No. 377, NACE, Houston, Texas.

Alonso, C., Andrade, C., Rodriguez, J., Casal, J. & Garcia, M. 1994. Rebar corrosion and time to cover cracking. *In concrete across borders international conference*, Odense, Denmark, pp. 301-319.

Alonso, C., Andrade, C., Rodriguez, J. & Diez, J. M. 1998. Factors controlling cracking of concrete affected by reinforcement corrosion. *Materials and Structures*, 31, August-September, pp. 435-441.

Andrade, C., Alonso, C. & Molina, F. J. 1993a. Cover cracking as a function of rebar corrosion: Part I – Experimental test. *Materials and Structures*, 26, pp. 453-464.

Andrade, C., Alonso, C. & Molina, F. J. 1993b. Cover cracking as a function of rebar corrosion: Part II – Numerical model. *Materials and Structures*, 26, pp. 532-548.

Andrade, C., Alonso, C., Rodriguez, J. & Casal, J. M. 1995. Relation between corrosion and concrete cracking. *Internal report* Brite/Euram BE-4062. DG XII, C.E.C.

Andrade, C., Alonso, C., Rodriguez, J. & Garcia, M. 1996. Cover cracking and amount of rebar corrosion: importance of the current applied accelerated tests. *In concrete repair, Rehabilitation and protection*, R. K. Dhir and M. R. Jones eds., E&FN Spon, London, UK, pp. 263-273.

Atimatay, E. & Ferguson, M. 1973 Early corrosion of reinforced concrete – A test report. *ACI Structural Journal*, 70, 9, pp. 606-611.

Bazant, Z. P. 1979. Physical model for steel corrosion in concrete sea structures – theory. *Journal Structural Division*, ASCE, 105, ST6, pp., 1137-1153.

Bazant, Z. P. 1979 Physical model for steel corrosion in concrete sea structures – application. *Journal Structural Division*, ASCE, 105, ST6, pp., 1155-1166.

Bedu, P. 1993. Volumetric changes of cement paste under exposure to the simulated corrosion products of steel and their influence on cracking susceptibility. M. Sc. Eng. Thesis, Florida Atlantic University, Boca Raton, Florida.

Beeby, A. W. 1983. Cracking, cover and corrosion of reinforcement. *Concrete International*, 5, 2, Pg. 35-40.

Fontana, M. G. 1986. *Corrosion engineering*. McGraw-Hill, 3rd ed., pp. 556, New York, New York, USA.

Harada, T., Idemitsu, T. & Watanabe, A. 1986. Demolition of concrete with expansive demolition agents. *Concrete library of Japanese Society of Civil Eng.*, 3 (360), pp. 63-81.

Harada, T., Soeda, K., Idemitsu, T. & Watanabe, A. 1993. Characteristics of expansive pressure and expansive demolition agent and the development of new pressure transducers, *Conc. Lib. JSCE*, 21 (478), pp. 95-109.

Leung, K. Y. 2001. Modeling of concrete cracking induced by steel expansion. *Journal of Materials in Civil Engineering*, May-June.

Liu, Y. & Weyers, R. E. 1995. Modeling the time to corrosion cracking in chloride contaminated reinforcement concrete structures. *ACI Materials Journal*, 95 (6), pp. 675-681.

Martín-Perez B. 1998. Service life modeling of RC highway structures exposed to chlorides". Ph.D. dissertation, Dept. of Civil Engineering, University of Toronto.

Noghabai, K. 1999. Discrete versus smeared versus element-embedded crack models on ring problem, J. Eng. Mechs., ASCE, 125 (3), pp. 307-315.

Ohtsu, M. & Yoshimura, S. 1997. Analysis of crack propagation and crack initiation due to corrosion reinforcement, Const. And Build. Mat., 11 (7-8), pp. 437-442.

Padovan, J. & Jae J. 1997. FE modeling of expansive oxide induced fracture of rebar reinforced concrete, *Engineering Fracture Mechanics*, 56 (6), pp. 797-812.

Pantazopoulou, S. J. & Papoulia, K. D. 2001. Modeling cover cracking due to reinforcement corrosion in RC structures. *Journal of Engineering Mechanics*. April.

Rasheeduzzafar, S., Al-Saadoun S. & Al-Gahtani, A. S. 1992. Corrosion cracking in relation to bar diameter cover and concrete quality. *Journal of Material in Civil Engineering*, Vol. 4 (4).

Reinhardt, H. W. 1984. *Fracture mechanics of an elastic softening material like concrete*. Heron (ed.). Vol. 29 No. 2.

Rodríguez, J., Ortega, L., Casal, J. & Diez, J. 1996. Corrosion reinforcement and service life of concrete structures, *Durab. Build. Mater. Compon.* 7 (1), pp. 117-126.

Sagoe-Crentsil, K. K. & Glasser, F. O. 1989a. Steel in concrete: Part I. A review of the electrochemical and thermodynamic aspects. *Magazine of Concrete Research*, 41, 149, pp. 205-212.

Sagoe-Crentsil, K. K. & Glasser, F. O. 1989b. Steel in concrete: Part II. Electron microscopy Analysis. *Magazine of Concrete Research*, 41, 149, pp. 213-220.

Sagoe-Crentsil, K. K. & Glasser, F. O. 1993. Constitution of green rust and its significance to the corrosion of steel in Portland cement. *Corrosion*, 49, 6, pp. 457-463.

Sagüés, A, and Torres A. 1998. “Concrete cover cracking and corrosion expansion of embedded reinforcing steel”. Proceedings of the third NACE Latin American region corrosion congress on rehabilitation of corrosion damaged infrastructures, Castro, P., Troconis, O. y Andrade, C. eds., pp. 215-229.

Tepfers, R. 1979. Cracking of concrete cover along anchored deformed reinforcing bars, *Mag. Conc. Res.*, 31 (106), pp. 3-12.

Timoshenko, S. 1989. *Strength of materials*, Espasa (ed.), Vol. II: Theory and complex problems, pp. 244.

Torres, A. 1999. Cracking induced by localized corrosion of reinforcement in chloride contaminated concrete. Ph. D. Thesis, University of South Florida, Florida, USA.

Tuutti, K. 1982. *Corrosion of steel in concrete*. Swedish Cement and Concrete Research Institute, Stockholm, Sweden.

Vidal, T., Castel, A. & Francois, R. 2004. Analyzing crack width to predict corrosion in reinforced concrete. *Cement and Concrete Research* 34, pp. 165-174.